Current Biology, Volume *23*

Supplemental Information

Discs Large Links Spindle Orientation to Apical-Basal Polarity in *Drosophila* Epithelia

Dan T. Bergstralh, Holly E. Lovegrove, and Daniel St Johnston

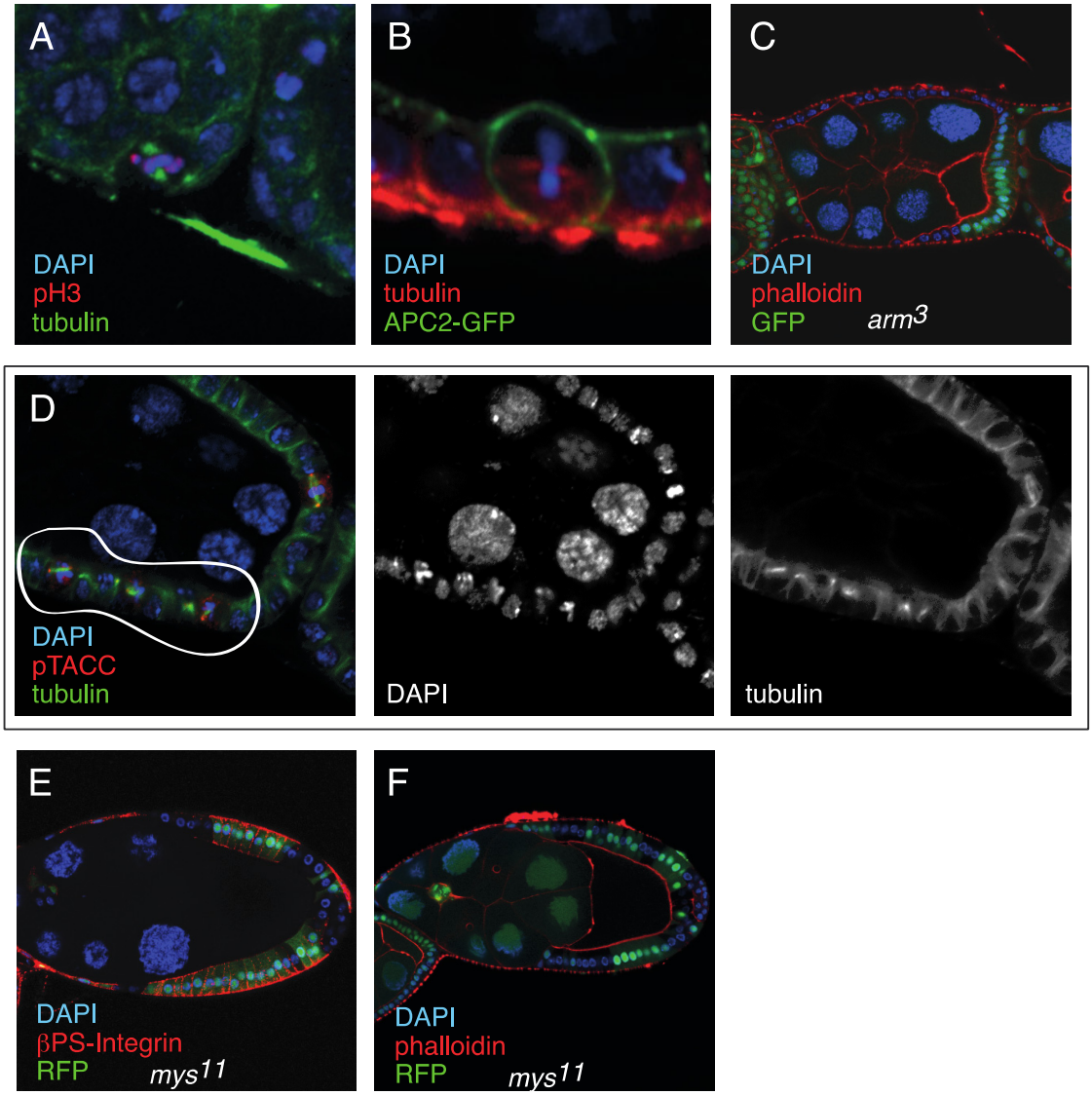

Figure S1. Related to Figure 1. Early stages of division in the follicle cell epithelium. **A)** A prometaphase cell in which the spindle is forming perpindicular to the epithelial sheet. Nascent spindle poles are stained with α–Tubulin (green). pH3 staining (red) confirms that the cell is mitotic. DAPI is shown in blue. **B)** APC-2-GFP (green) is not restricted to adherens junctions in

mitotic follicle cells. **C)** Armadillo is important but not necessary for maintainence of epithelial integrity. *arm*^{3} mutant cells (marked by the absence of GFP) may be flattened or lost but are often normal in appearance. **D)** The spindle is assembled before it achieves its final orientation. Several cells outlined by the white line are in pro-metaphase, as indicated by anti-pTACC *(*Transforming Acidic Coiled-Coil) staining (which marks only mitotic centrosomes) but only partially condensed chromatin. Tubulin staining demonstrates that spindles are being assembled in these cells before the centrosomes reach their metaphase orientation. For comparison, see the metaphase cell in the upper right. **E)** *mys*^{11} is a protein null allele. Immunoreactivity to an anti-βPS Integrin antibody is lost in *mys*^{11} mutant clones (marked by the absence of RFP in green). **F)** As reported previously, *mys*^{11} mutant clones cause disorganization of the follicle cell epithelium, particualrly at the poles of the egg chamber.

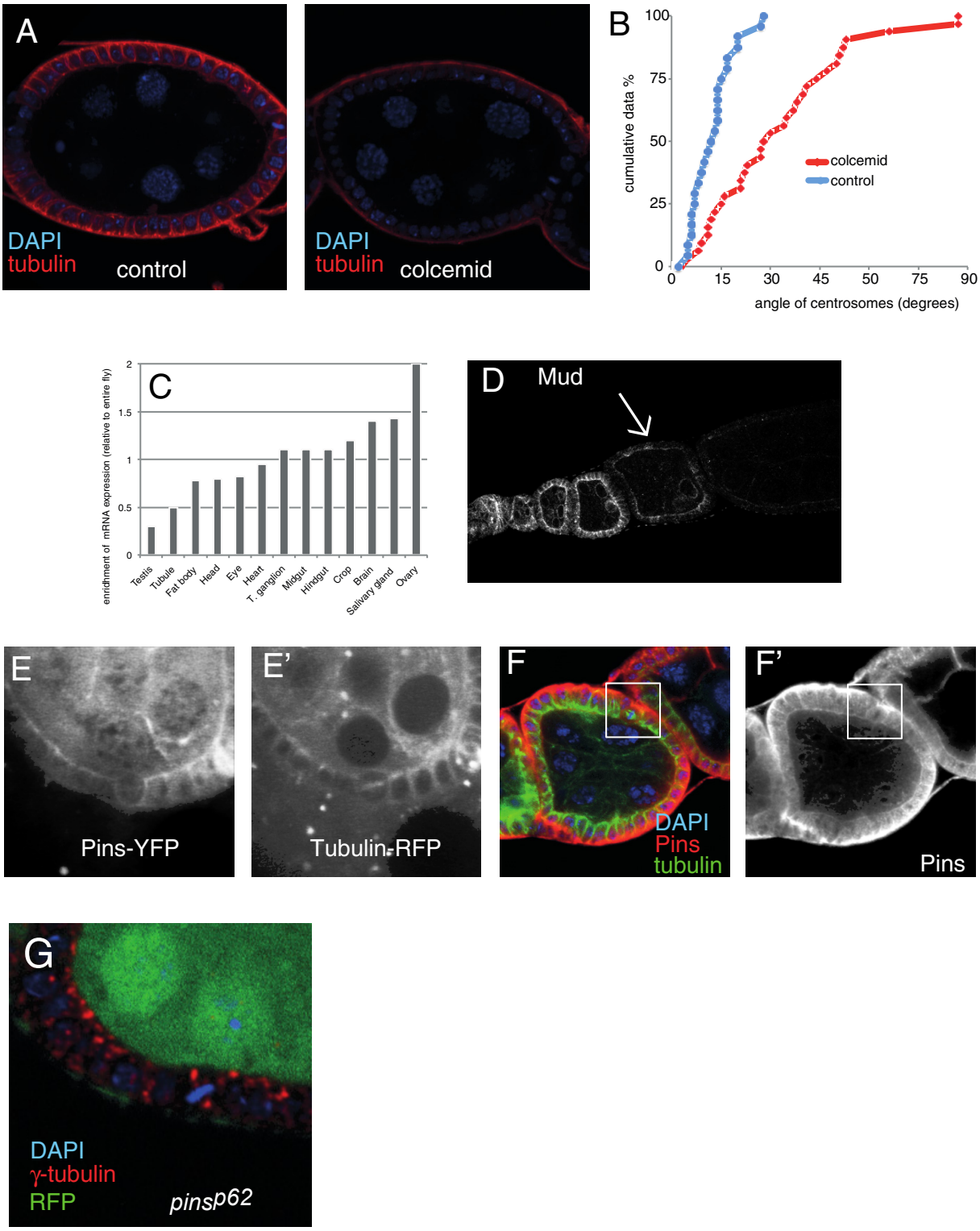

Figure S2. Related to Figure 3. Pins localization and activity in follicle cells. **A)** Colcemid treatment dissolves follicle mictrotubules. Egg chambers were incubated for one hour in Schneider's medium with or without colcemid, then stained for tubulin (in red) and examined at the same laser intensity. Some background staining remains outside the egg chamber following colcemid treatment but the specific microtubule signal within the follicle cells is lost **B)** A

cumulative plot of centrosomal angles with or without colcemid treatment. For these experiments, we drew a line connecting the two centrosomes in a metaphase cell and measured the angle of this line relative to the two apical corners of the cell. These angles differ with a *p* value of < 0.005 as determined by the Kolmogorov-Smirnov test. **C)** *pins* mRNA is most highly enriched in the ovaries of the adult fly. Expression is shown as enrichment relative to the entire fly. Data was mined from FlyAtlas. (T. ganglion = Thoracicoabdominal ganglion). **D)** Mud is expressed in follicle cells in early stage egg chambers. Staining disappears after stage 6 (marked by arrow). **E)** Pins-YFP (E) localises around the basolateral cortex of mitotic cells but is apical in interphase. RFP-Tubulin (E') identifies the mitotic spindle and thus the mitotic cell. **F)** Anti-Pins staining in the egg chamber demonstrates the lateral localisation of Pins during mitosis. We attribute the strong basal signal to poor antibody penetration in this tissue. The white box outlines a mitotic cell. **G)** Centrosomes (as marked by anti-γ-tubulin staining in red) are not disrupted in $pins^{p62}$ clones (marked by the absence of GFP).

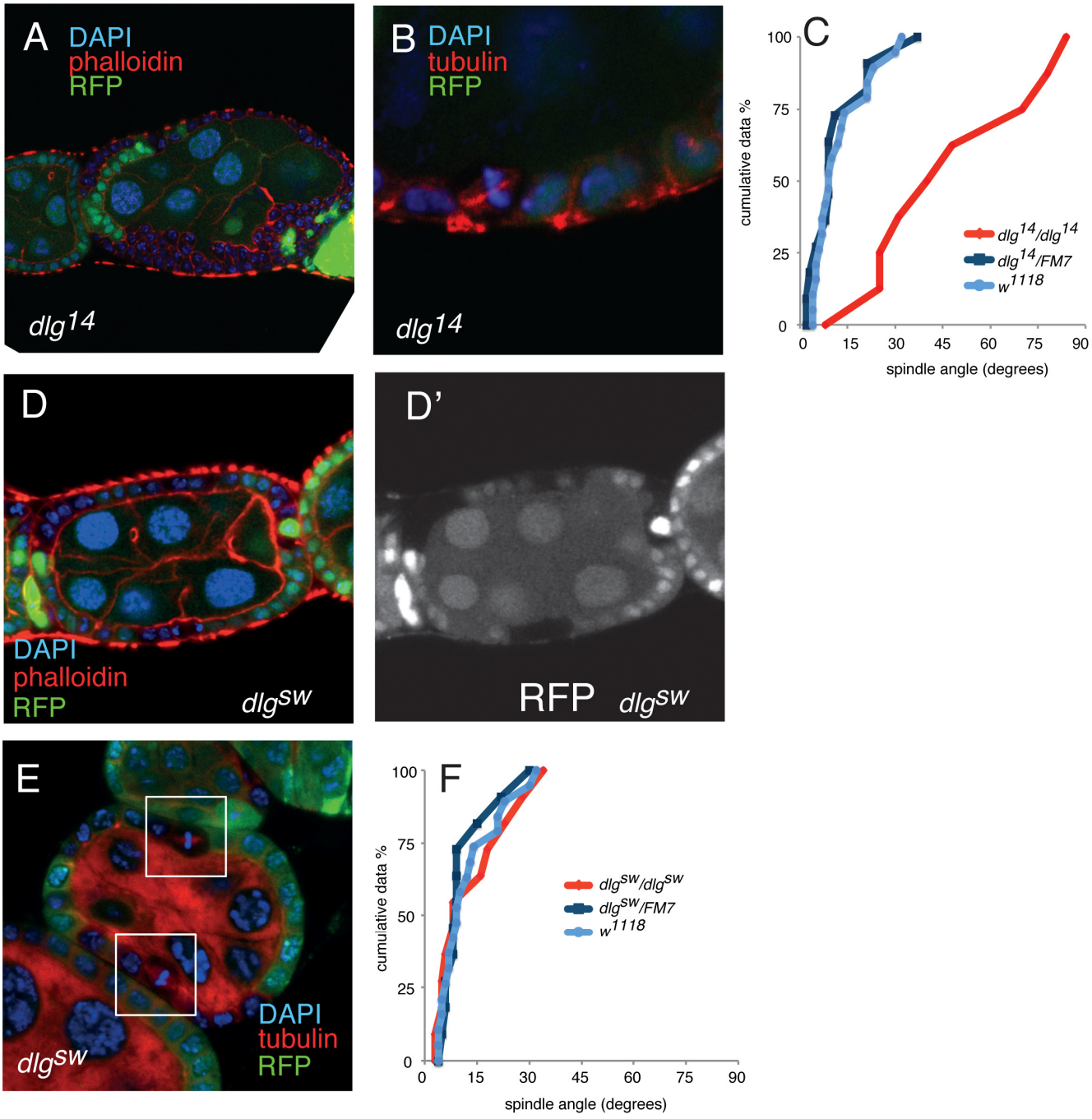

Figure S3. Related to Figure 4. *discs large* alleles have different effects on spindle orientation and epithelial organization. **A)** As expected, dlg^{14} clones (marked by the absence of RFP in green) demonstrate a loss of epithelial polarity, rounded morphology, and overproliferation. **B)** Metaphase spindles are randomized in single layer dlg^{14} clones. **C)** A cumulative plot of metaphase spindle angles in dlg^{14} mutant follicle cells. **D** and **D'**) Epithelial organization is not disrupted in dlg^{sw} mutant follicle cell clones. Clones are marked by the absence of RFP (green in D, grey in D'). Phalloidin in red, DAPI in blue. **E)** Metaphase spindles are not misoriented in dlg^{sw} mutant follicle cells (marked by the absence of GFP). **F)** A cumulative plot of spindle angles in dlg^{sw} mutant follicle cells.

Supplemental Experimental Procedures

***Drosophila* stocks**: The following mutant alleles and transgenic constructs have been described previously: *mys*^{11} [1], *pins*^{p62} [2], *mud*^{2} and *mud*^{3} [3], *apc*^{q8}, *apc*^{g10} [4], *arm*^{3} [5], *dlg*^{14} and *dlg*^{18} [6], *dlg*^{sw} [7], *Ubq*-Pins-YFP, *pins*^{p62} [8], *apkc*^{psu141} [9], *apkc*^{k06403} [10], *apkc*^{ts} [11], *Ubq*-Sas4-GFP [12], Bazooka-GFP [13], and Crumbs-GFP [14]. *dlg*^{18} FRT19A was a generous gift from Floris Bosveld of the Bellaïche lab. *dlg*^{14} FRT19A and *arm*^{3} FRT19A were generated by Aram Sayadian of the St Johnston lab. FRT82B *pins*^{p62} and *dlg*^{sw} FRT19A were generated by D. Bergstralh. Dlg-YFP was generated in a protein trap screen [15]. The following background stocks were used to generate mitotic clones, which were induced by heat shock at 37° for multiple periods of two hours: RFP-nls, hsflp, FRT19A and hsflp;FRT40A GFP-nls, and hsflp;;FRT82B GFP-nls.

Reagents: The following antibodies were used in this study: rabbit anti-phospho-H3 (Cell Signaling), rabbit anti-aPKC (Santa Cruz), mouse anti-Armadillo, anti-βPS Integrin, and anti-Dlg (Developmental Studies Hybridoma Bank), rabbit anti-Centrosomin and rabbit anti-pTACC (gift from J. Raff), rabbit anti-Mud (gift from H. Nash), mouse anti-α-tubulin and anti-γ-tubulin (Sigma). Anti-Pins was generated against full length Pins protein. Rhodamine-Phalloidin was purchased from Invitrogen. Vectashield with DAPI was purchased from Vector Labs. Conjugated secondary antibodies were purchased from Jackson Immunoresearch.

Expression data: Cross-tissue expression of *pins* mRNA was mined from FlyAtlas (flyatlas.org).

Spindle angle measurements: Centrosome angles were calculated using Image J. The angle of a line drawn connecting the two centrosomes was determined relative to a line drawn connecting the adherens junctions at the two apical corners of the mitotic cell. These corners are shared by this cell and its neighbours.

Statistics: The Kolmogorov-Smirnov test was performed using the calculator provided by Tom Kirkman at http://www.physics.csbsju.edu/stats/KS-test.html. The test for normal distribution was performed using NormQuant by Scott Guth.

Supplemental References

1. Zusman, S., Patel-King, R. S., Ffrench-Constant, C., and Hynes, R. O. (1990). Requirements for integrins during Drosophila development. Development *108*, 391–402.

2. Yu, F., Morin, X., Cai, Y., Yang, X., and Chia, W. (2000). Analysis of partner of inscuteable, a novel player of Drosophila asymmetric divisions, reveals two distinct steps in inscuteable apical localization. Cell *100*, 399–409.

3. Yu, J. X., Guan, Z., and Nash, H. A. (2006). The mushroom body defect gene product is an essential component of the meiosis II spindle apparatus in Drosophila oocytes. Genetics *173*, 243–253.

4. McCartney, B. M., Price, M. H., Webb, R. L., Hayden, M. A., Holot, L. M., Zhou, M., Bejsovec, A., and Peifer, M. (2006). Testing hypotheses for the functions of APC family proteins using null and truncation alleles in Drosophila. Development *133*, 2407–2418.

5. Peifer, M., Rauskolb, C., Williams, M., Riggleman, B., and Wieschaus, E. (1991). The segment polarity gene armadillo interacts with the wingless signaling pathway in both embryonic and adult pattern formation. Development *111*, 1029–1043.

6. Woods, D. F., and Bryant, P. J. (1989). Molecular cloning of the lethal(1)discs large-1 oncogene of Drosophila. Developmental Biology *134*, 222–235.

7. Woods, D. F., and Bryant, P. J. (1991). The discs-large tumor suppressor gene of Drosophila encodes a guanylate kinase homolog localized at septate junctions. Cell *66*, 451–464.

8. David, N. B., Martin, C. A., Segalen, M., Rosenfeld, F., Schweisguth, F., and Bellaïche, Y. (2005). Drosophila Ric-8 regulates Galphai cortical localization to promote Galphai-dependent planar orientation of the mitotic spindle during asymmetric cell division. Nat Cell Biol *7*, 1083–1090.

9. Kim, S., Gailite, I., Moussian, B., Luschnig, S., Goette, M., Fricke, K., Honemann-Capito, M., Grubmüller, H., and Wodarz, A. (2009). Kinase-activity-independent functions of atypical protein kinase C in Drosophila. J Cell Sci *122*, 3759–3771.

10. Wodarz, A., Ramrath, A., Grimm, A., and Knust, E. (2000). Drosophila atypical protein kinase C associates with Bazooka and controls polarity of epithelia and neuroblasts. Journal of Cell Biology *150*, 1361–1374.

11. Guilgur, L. G., Prudencio, P., Ferreira, T., Pimenta-Marques, A. R., and Martinho, R. G. (2012). Drosophila aPKC is required for mitotic spindle orientation during symmetric division of epithelial cells. Development *139*, 503–513.

12. Peel, N., Stevens, N. R., Basto, R., and Raff, J. W. (2007). Overexpressing centriole-replication proteins in vivo induces centriole overduplication and de novo formation. Current Biology *17*, 834–843.

13. Benton, R., and St Johnston, D. (2003). A conserved oligomerization domain in

drosophila Bazooka/PAR-3 is important for apical localization and epithelial polarity. Current Biology *13*, 1330–1334.

14. Huang, J., Zhou, W., Dong, W., Watson, A. M., and Hong, Y. (2009). From the Cover: Directed, efficient, and versatile modifications of the Drosophila genome by genomic engineering. Proc Natl Acad Sci USA *106*, 8284–8289.

15. Rees, J. S., Lowe, N., Armean, I. M., Roote, J., Johnson, G., Drummond, E., Spriggs, H., Ryder, E., Russell, S., St Johnston, D., et al. (2011). In vivo analysis of proteomes and interactomes using Parallel Affinity Capture (iPAC) coupled to mass spectrometry. Mol. Cell Proteomics *10*, M110.002386.